

Fully strange tetraquark states via QCD sum rules

Bing-Dong Wan^{1,2*} and Ji-Chong Yang^{1,2†}

¹*Department of Physics, Liaoning Normal University, Dalian 116029, China*

²*Center for Theoretical and Experimental High Energy Physics,
Liaoning Normal University, Dalian 116029, China*

Abstract

In this paper, we have systematically explored the mass spectrum of fully strange tetraquark candidates within the framework of QCD sum rules, focusing on states with quantum numbers $J^{PC} = 0^{++}$, 0^{-+} , 0^{--} , 1^{--} , 1^{+-} , and 1^{++} . The analysis reveals the existence of fully strange tetraquark states with masses ranging from approximately 2.08 to 3.12 GeV. These predictions are confronted with existing experimental observations of potential fully strange tetraquark resonances, notably the $X(2300)$ recently reported by the BESIII Collaboration, which may be interpreted as a fully strange tetraquark state. Furthermore, the possible decay modes of these fully strange tetraquark states are analyzed, providing guidance for their identification in current and future high energy experiments such as BESIII, Belle II, and LHCb.

* wanbd@lnnu.edu.cn

† yangjichong@lnnu.edu.cn

I. INTRODUCTION

The study of novel hadronic states—such as multiquarks, hybrids, and glueballs—has gained significant attention in recent years as experimental and theoretical advances continue to challenge the conventional quark model [1, 2]. Since the discovery of the $X(3872)$ state [3], more than thirty similar novel states or candidates have been reported in various experiments. This growing list of observations strongly suggests that many more new hadronic states are likely to be discovered in the near future, marking what can be regarded as a renaissance in hadron spectroscopy. Unraveling the internal structure and underlying dynamics of these newly observed states constitutes one of the most compelling and significant challenges in contemporary hadron physics.

In the light hadron sector, the identification of novel hadronic states remains a significant challenge, primarily due to the small mass splittings between states and the resulting strong mixing among them. This often obscures the distinction between novel and conventional configurations in experimental analyses, except the novel hadronic states possessing exotic quantum numbers, which are forbidden in the conventional quark model, offer cleaner signatures for identifying nontraditional structures. However, with the rapid accumulation of high-precision experimental data in the charm quark sector, the BESIII experiment is now well-positioned to conduct a systematic investigation of hadronic phenomena in this energy region—including, crucially, the search for and study of light novel hadrons [4–13].

Among the various novel hadron candidates, fully strange tetraquark states—composed entirely of two strange quarks and two strange antiquarks ($ss\bar{s}\bar{s}$)—constitute a particularly intriguing and theoretically clean subclass. Owing to their flavor purity, these states are free from mixing with light (u, d) or heavy (c, b) quark components, thereby offering a uniquely controlled environment for investigating fundamental aspects of QCD, including quark confinement, color dynamics, and gluon-mediated interactions. Their distinct quark content also enhances their stability against decay into lighter mesons via quark flavor rearrangement. Notably, fully strange tetraquarks can accommodate exotic quantum numbers—such as $J^{PC} = 0^{--}$ —which are strictly forbidden in conventional quark–antiquark meson configurations. The observation of such states would thus serve as a clear indication of multiquark

dynamics beyond the conventional hadron classification scheme.

Recently, the BESIII Collaboration reported the observation of a resonant structure, denoted as $X(2300)$, in a partial wave analysis of the process $\psi(3686) \rightarrow \phi\eta\eta'$ [14]. The structure appears prominently in the $\phi\eta$ and $\phi\eta'$ invariant mass spectra, with statistical significances of 9.6σ and 5.6σ , respectively, and the measured decay width of the state is approximately 89 MeV. The measured mass of the $X(2300)$ exhibits a notable discrepancy with the theoretical predictions for conventional strangeonium states as reported in Refs. [15–21]. In contrast, the mass of the fully strange tetraquark state with quantum numbers $J^{PC} = 1^{+-}$, as calculated in Ref. [22], shows good agreement with the observed mass of the $X(2300)$, suggesting a possible tetraquark interpretation.

Motivated by the observation of the $X(2300)$ resonance, fully strange tetraquark states have attracted renewed attention, especially through the lens of QCD sum rule analyses [23], which provide a nonperturbative framework for exploring their possible structure and mass spectrum. QCD sum rules (QCDSR) constitute a QCD-based theoretical framework that systematically incorporates nonperturbative effects. This approach has been successfully applied to a wide range of problems in hadron spectroscopy, providing valuable insights into the structure and properties of conventional and novel hadrons [24–62]. The initial step in formulating QCD sum rules involves constructing appropriate interpolating currents that correspond to the hadrons under investigation. These currents encode essential information about the hadrons, such as their quantum numbers and internal structural components. Based on these interpolating currents, the two-point correlation function is defined, which admits two distinct representations: the operator product expansion (OPE) side and the phenomenological side. By matching these two representations through a dispersion relation and applying quark-hadron duality, the QCD sum rules are established. This framework then enables the extraction of hadronic properties, such as the mass spectrum, from the underlying QCD dynamics.

In this work, the masses of the fully strange tetraquark states in molecular configurations with $J^{PC} = 0^{++}$, 0^{-+} , 0^{--} , 1^{--} , 1^{+-} , and 1^{++} are investigated within the framework of QCD sum rules. Since the 1^{-+} states were investigated in our previous work [24], and the

0^{+-} state does not admit a molecular configuration, these two states are excluded from the present analysis. The organization of the paper is as follows. Following the Introduction, a concise overview of the QCD sum rules framework and the essential formulas employed in our calculations are presented in Sec.II. The numerical analysis and corresponding results are discussed in Sec.III. The possible tetraquark decay modes are given in Sec.cIV. Finally, a brief summary and concluding remarks are provided in the last section.

II. FORMALISM

To evaluate the mass spectrum of fully strange tetraquark states within the QCD sum rule framework, the initial step is to construct suitable interpolating currents. The procedure for constructing these currents is as follows. First, all possible currents are listed, specifying their constituent quark content and corresponding Dirac gamma matrix structures. Subsequently, parity (P) and charge conjugation (C) transformations are applied to these currents to identify their transformation properties. By selecting the currents with the desired quantum numbers J^{PC} and eliminating redundant currents via Fierz rearrangements, a complete and non-redundant set of interpolating currents is obtained.

Via the aforementioned procedure, the interpolating currents for fully strange tetraquark states with $J^{PC} = 0^{++}$ in molecular configurations are constructed in the following forms:

$$j_{0^{++}}^A(x) = [\bar{s}_a(x)\gamma_5 s_a(x)][\bar{s}_b(x)\gamma_5 s_b(x)] , \quad (1)$$

$$j_{0^{++}}^B(x) = [\bar{s}_a(x)s_a(x)][\bar{q}_b(x)q_b(x)] , \quad (2)$$

$$j_{0^{++}}^C(x) = [\bar{s}_a(x)\gamma_\mu s_a(x)][\bar{s}_b(x)\gamma_\mu s_b(x)] , \quad (3)$$

$$j_{0^{++}}^D(x) = [\bar{s}_a(x)\gamma_\mu\gamma_5 s_a(x)][\bar{s}_b(x)\gamma_\mu\gamma_5 s_b(x)] , \quad (4)$$

$$j_{0^{++}}^E(x) = [\bar{s}_a(x)\sigma_{\mu\nu}s_a(x)][\bar{s}_b(x)\sigma_{\mu\nu}s_b(x)] , \quad (5)$$

where the subscripts a and b are color indices.

The interpolating currents for fully strange tetraquark states with $J^{PC} = 0^{-+}$ in molec-

ular configurations are constructed in the following forms:

$$j_{0-+}^A(x) = i[\bar{s}_a(x)\gamma_5 s_a(x)][\bar{s}_b(x)s_b(x)] , \quad (6)$$

$$j_{0-+}^B(x) = i[\bar{s}_a(x)\sigma_{\mu\nu}s_a(x)][\bar{s}_b(x)\sigma_{\mu\nu}\gamma_5 s_b(x)] . \quad (7)$$

The interpolating currents for fully strange tetraquark states with $J^{PC} = 0^{--}$ in molecular configurations are constructed in the following forms:

$$j_{0--}^A(x) = i[\bar{s}_a(x)\gamma_\mu\gamma_5 s_a(x)][\bar{s}_b(x)\gamma_\mu s_b(x)] . \quad (8)$$

The interpolating currents for fully strange tetraquark states with $J^{PC} = 1^{--}$ in molecular configurations are constructed in the following forms:

$$j_{1--}^{A,\mu}(x) = i[\bar{s}_a(x)s_a(x)][\bar{s}_b(x)\gamma_\mu s_b(x)] , \quad (9)$$

$$j_{1--}^{B,\mu}(x) = i[\bar{s}_a(x)\sigma_{\mu\nu}\gamma_5 s_a(x)][\bar{s}_b(x)\gamma_\nu\gamma_5 s_b(x)] . \quad (10)$$

The interpolating currents for fully strange tetraquark states with $J^{PC} = 1^{+-}$ in molecular configurations are constructed in the following forms:

$$j_{1+-}^{A,\mu}(x) = i[\bar{s}_a(x)\gamma_5 s_a(x)][\bar{s}_b(x)\gamma_\mu s_b(x)] , \quad (11)$$

$$j_{1+-}^{B,\mu}(x) = i[\bar{s}_a(x)\sigma_{\mu\nu}s_a(x)][\bar{s}_b(x)\gamma_\nu\gamma_5 s_b(x)] . \quad (12)$$

The interpolating currents for fully strange tetraquark states with $J^{PC} = 1^{++}$ in molecular configurations are constructed in the following forms:

$$j_{1++}^{A,\mu}(x) = i[\bar{s}_a(x)s_a(x)][\bar{s}_b(x)\gamma_\mu\gamma_5 s_b(x)] , \quad (13)$$

$$j_{1++}^{B,\mu}(x) = i[\bar{s}_a(x)\sigma_{\mu\nu}\gamma_5 s_a(x)][\bar{s}_b(x)\gamma_\nu s_b(x)] . \quad (14)$$

With the currents (1)-(14), the two-point correlation function can be readily established, i.e.,

$$\Pi_{J^{PC}}^k(q^2) = i \int d^4x e^{iq \cdot x} \langle 0 | T \{ j_{J^{PC}}^k(x), j_{J^{PC}}^k(0)^\dagger \} | 0 \rangle , \quad (15)$$

$$\Pi_{J^{PC}, \mu\nu}^k(q^2) = i \int d^4x e^{iq \cdot x} \langle 0 | T \{ j_{J^{PC}}^{k,\mu}(x), j_{J^{PC}}^{k,\nu}(0)^\dagger \} | 0 \rangle . \quad (16)$$

Here, $\Pi(q^2)$ and $\Pi_{\mu\nu}(q^2)$ denote the correlation functions corresponding to states with spin $J = 0$ and 1, respectively, the index k runs from A to E for 0^{++} states, takes the value A for 0^{--} state, and runs from A to B in other case, and $|0\rangle$ denotes the physical vacuum. The correlation function $\Pi_{\mu\nu}(q^2)$ corresponding to spin $J = 1$ states can be expressed in the following Lorentz-covariant form:

$$\Pi_{\mu\nu}(q^2) = -\left(g_{\mu\nu} - \frac{q_\mu q_\nu}{q^2}\right)\Pi_1(q^2) + \frac{q_\mu q_\nu}{q^2}\Pi_0(q^2), \quad (17)$$

where the subscripts 1 and 0, respectively, denote the quantum numbers of the spin 1 and 0 mesons.

On the phenomenological side, the correlation function $\Pi(q^2)$ can be represented as a dispersion integral over the physical spectrum, with the ground-state tetraquark contribution explicitly isolated, i.e.,

$$\Pi_{JPC}^{phen, k}(q^2) = \frac{(\lambda_{JPC}^k)^2}{(M_{JPC}^k)^2 - q^2} + \frac{1}{\pi} \int_{s_0}^{\infty} ds \frac{\rho_{JPC}^k(s)}{s - q^2}, \quad (18)$$

where M denotes the mass of the tetraquark state, λ is the coupling constant of the hadron, and $\rho(s)$ represents the spectral density, which encapsulates the contributions from higher excited states and the continuum above the threshold s_0 .

In the OPE representation, the correlation function $\Pi(q^2)$ can be expressed through a dispersion relation as follows:

$$\Pi_{JPC}^{OPE, k}(q^2) = \int_{s_{min}}^{\infty} ds \frac{\rho_{JPC}^{OPE, k}(s)}{s - q^2} + \Pi_{JPC}^{sum, k}(q^2). \quad (19)$$

Here, s_{min} denotes the kinematic threshold, which typically corresponds to the squared sum of the current-quark masses of the hadron [25]. Π^{sum} represents the contributions to the correlation function that do not possess an imaginary part but yield nontrivial terms after the Borel transformation. The spectral density is given by $\rho^{OPE}(s) = \text{Im}[\Pi^{OPE}(s)]/\pi$, and

$$\begin{aligned} \rho^{OPE}(s) = & \rho^{pert}(s) + \rho^{\langle \bar{s}s \rangle}(s) + \rho^{\langle G^2 \rangle}(s) + \rho^{\langle \bar{s}Gs \rangle}(s) \\ & + \rho^{\langle \bar{s}s \rangle^2}(s) + \rho^{\langle G^2 \rangle \langle \bar{s}s \rangle}(s) + \rho^{\langle \bar{s}s \rangle \langle \bar{s}Gs \rangle}(s). \end{aligned} \quad (20)$$

To calculate the spectral density on the OPE side, as given in Eq. (20), the full light-quark

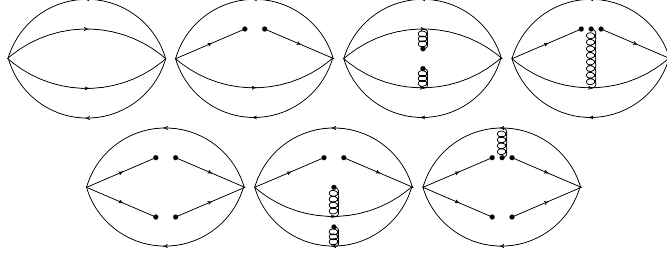


FIG. 1: The typical Feynman diagrams related to the correlation function, where the solid lines stand for the quarks and the spiral ones for gluons.

propagator $S_{ij}^q(x)$ is utilized, namely,

$$S_{ij}^q(x) = \frac{i\delta_{ij}\not{x}}{2\pi^2x^4} - \frac{\delta_{ij}m_q}{4\pi^2x^2} - \frac{it_{ij}^a G_{\alpha\beta}^a}{2^5\pi^2x^2}(\sigma^{\alpha\beta}\not{x} + \not{x}\sigma^{\alpha\beta}) - \frac{\delta_{ij}}{12}\langle\bar{q}q\rangle + \frac{i\delta_{ij}\not{x}}{48}m_q\langle\bar{q}q\rangle - \frac{\delta_{ij}x^2}{192}\langle g_s\bar{q}\sigma\cdot Gq\rangle \\ + \frac{i\delta_{ij}x^2\not{x}}{2^7\times 3^2}m_q\langle g_s\bar{q}\sigma\cdot Gq\rangle - \frac{t_{ij}^a\sigma_{\alpha\beta}}{192}\langle g_s\bar{q}\sigma\cdot Gq\rangle + \frac{it_{ij}^a}{768}(\sigma_{\alpha\beta}\not{x} + \not{x}\sigma_{\alpha\beta})m_q\langle g_s\bar{q}\sigma\cdot Gq\rangle, \quad (21)$$

where the vacuum condensates are explicitly exhibited. For a more detailed discussion of the quark propagator, readers are referred to Refs. [25, 26]. The Feynman diagrams corresponding to the various terms in Eq.(20) are schematically illustrated in Fig. 1.

By applying the Borel transformation to Eqs.(18) and(19), and equating the OPE representation with the phenomenological side of the correlation function $\Pi(q^2)$, one can derive the mass of the tetraquark state as:

$$M_{JPC}^k(s_0, M_B^2) = \sqrt{-\frac{L_{JPC,1}^k(s_0, M_B^2)}{L_{JPC,0}^k(s_0, M_B^2)}}. \quad (22)$$

Here L_0 and L_1 are respectively defined as

$$L_{JPC,0}^k(s_0, M_B^2) = \int_{s_{min}}^{s_0} ds \rho_{JPC}^{OPE,k}(s)e^{-s/M_B^2} + \Pi_{JPC}^{sum,k}(M_B^2), \quad (23)$$

and

$$L_{JPC,1}^k(s_0, M_B^2) = \frac{\partial}{\partial \frac{1}{M_B^2}} L_{JPC,0}^k(s_0, M_B^2). \quad (24)$$

III. NUMERICAL ANALYSIS

In the numerical analysis, we adopt widely accepted input parameters as reported in Refs. [27–32], namely: $m_u = 2.16_{-0.26}^{+0.49}$ MeV, $m_d = 4.67_{-0.17}^{+0.48}$ MeV, $m_s = (95 \pm 5)$ MeV,

$$\langle \bar{q}q \rangle = -(0.23 \pm 0.03)^3 \text{ GeV}^3, \langle \bar{s}s \rangle = (0.8 \pm 0.1) \langle \bar{q}q \rangle, \langle \bar{q}g_s \sigma \cdot Gq \rangle = m_0^2 \langle \bar{q}q \rangle, \langle \bar{s}g_s \sigma \cdot Gs \rangle = m_0^2 \langle \bar{s}s \rangle, \langle g_s^2 G^2 \rangle = (0.88 \pm 0.25) \text{ GeV}^4, \text{ and } m_0^2 = (0.8 \pm 0.2) \text{ GeV}^2.$$

Moreover, two additional parameters, s_0 and M_B^2 are introduced in the process of establishing the QCD sum rules. These parameters are determined following the standard procedure by satisfying two well-established criteria [23, 25, 30–32]. The first criterion concerns the convergence of the operator product expansion (OPE), which is ensured by examining the relative contributions of higher-dimensional condensates to the total OPE. A suitable Borel window for M_B^2 is selected such that the OPE remains convergent in the chosen region. The second criterion requires that the pole contribution (PC) from the ground state should dominate over the continuum, typically accounting for more than 50% of the total spectral density [23, 31, 32]. These two criteria can be mathematically expressed as:

$$R^{OPE} = \left| \frac{L_0^{dim=8}(s_0, M_B^2)}{L_0(s_0, M_B^2)} \right|, \quad (25)$$

$$R^{PC} = \frac{L_0(s_0, M_B^2)}{L_0(\infty, M_B^2)}. \quad (26)$$

To determine an appropriate value for the continuum threshold s_0 , we follow a procedure analogous to that employed in Refs. [25, 30, 32]. In this approach, the goal is to identify an optimal value of s_0 that yields a stable Borel window for the extracted mass of the fully strange tetraquark state. Within this window, the mass prediction should exhibit minimal dependence on the Borel parameter M_B^2 , ensuring the reliability of the QCD sum rule analysis. In practical calculations, $\sqrt{s_0}$ is varied by 0.1 GeV around a central value to determine the corresponding lower and upper bounds, and hence the uncertainties of $\sqrt{s_0}$ [25].

With the aforementioned preparations, the mass spectrum of the light tetraquark states can now be evaluated numerically. For the current $J_{0^{++}}^A$, the OPE convergence ratio $R_{A,0^{++}}^{OPE}$ and the pole contribution ratio $R_{A,0^{++}}^{PC}$ are plotted as functions of the Borel parameter M_B^2 in Fig.2(a), for three different values of the continuum threshold $\sqrt{s_0} = 2.8, 2.9$, and 3.0 GeV. The dependence of the extracted mass $M_{0^{++}}^A$ on the Borel parameter is illustrated in Fig.2(b). From these analyses, an optimal Borel window is identified as $1.4 \leq M_B^2 \leq 2.2 \text{ GeV}^2$, within which both the OPE convergence and pole dominance criteria are satisfied. Accordingly, the

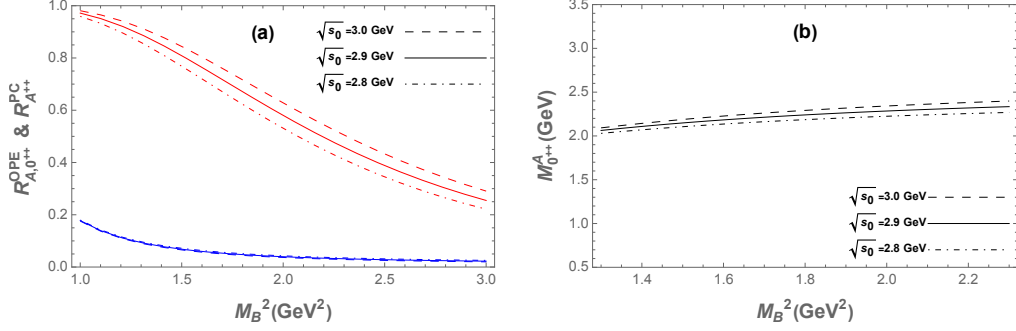


FIG. 2: (a) The ratios $R_{A,0^{++}}^{OPE}$ and $R_{A,0^{++}}^{PC}$ as functions of the Borel parameter M_B^2 for different values of $\sqrt{s_0}$ for current (1), where blue lines represent $R_{A,0^{++}}^{OPE}$ and red lines denote $R_{A,0^{++}}^{PC}$. (b) The mass of 0^{++} fully strange tetraquark state as a function of the Borel parameter M_B^2 for different values of $\sqrt{s_0}$.

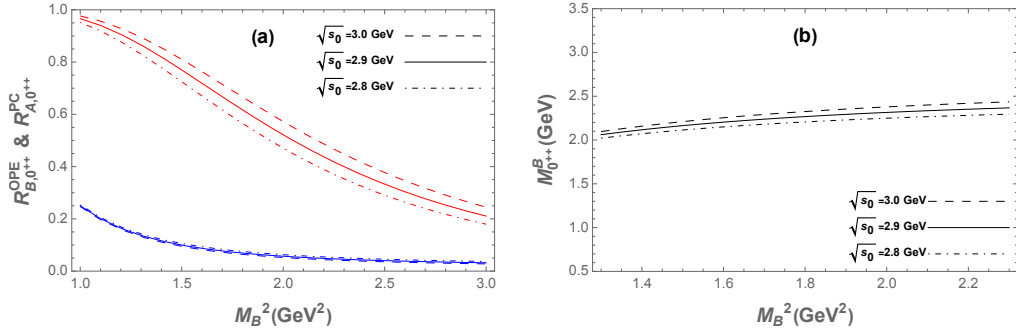


FIG. 3: (a) The ratios $R_{B,0^{++}}^{OPE}$ and $R_{B,0^{++}}^{PC}$ as functions of the Borel parameter M_B^2 for different values of $\sqrt{s_0}$ for current (2), where blue lines represent $R_{B,0^{++}}^{OPE}$ and red lines denote $R_{B,0^{++}}^{PC}$. (b) The mass of 0^{++} fully strange tetraquark state as a function of the Borel parameter M_B^2 for different values of $\sqrt{s_0}$.

mass of the fully strange tetraquark state corresponding to the current $J_{0^{++}}^A$ is extracted to be:

$$M_{0^{++}}^A = (2.35 \pm 0.15) \text{ GeV}. \quad (27)$$

For the current $J_{0^{++}}^B$, the OPE convergence and pole contribution ratios, $R_{B,0^{++}}^{OPE}$ and $R_{A,0^{++}}^{PC}$ are illustrated as functions of the Borel parameter M_B^2 in Fig.3(a), with continuum thresholds $\sqrt{s_0} = 2.8, 2.9$, and 3.0 GeV. The corresponding Borel stability curve of the

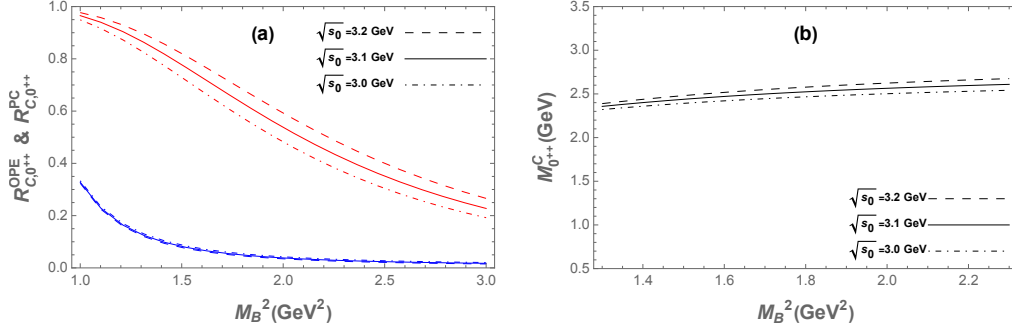


FIG. 4: (a) The ratios $R_{C,0^{++}}^{OPE}$ and $R_{C,0^{++}}^{PC}$ as functions of the Borel parameter M_B^2 for different values of $\sqrt{s_0}$ for current (3), where blue lines represent $R_{C,0^{++}}^{OPE}$ and red lines denote $R_{C,0^{++}}^{PC}$. (b) The mass of 0^{++} fully strange tetraquark state as a function of the Borel parameter M_B^2 for different values of $\sqrt{s_0}$.

extracted mass $M_{0^{++}}^B$ is shown in Fig.3(b). An optimal Borel window is identified as $1.4 \leq M_B^2 \leq 2.1$ GeV², where the standard criteria of OPE convergence and pole dominance are well satisfied. Within this window, the predicted mass is:

$$M_{0^{++}}^B = (2.24 \pm 0.16) \text{ GeV}. \quad (28)$$

For the current $J_{0^{++}}^C$, the ratios, $R_{C,0^{++}}^{OPE}$ and $R_{C,0^{++}}^{PC}$ as functions of M_B^2 are plotted in Fig.4(a) for several values of $\sqrt{s_0} = 3.0, 3.1$, and 3.2 GeV. The dependence of the resulting mass $M_{0^{++}}^C$ on the Borel parameter is displayed in Fig.4(b). The valid Borel window is determined to be $1.4 \leq M_B^2 \leq 2.1$ GeV², within which the mass of the fully strange tetraquark state is evaluated as:

$$M_{0^{++}}^C = (2.50 \pm 0.14) \text{ GeV}. \quad (29)$$

For the current $J_{0^{++}}^D$, we show the convergence and pole contributions in Fig.5(a), and the mass curve in Fig.5(b) with $\sqrt{s_0} = 3.0, 3.1$, and 3.2 GeV. A stable mass prediction is obtained within the Borel window $1.4 \leq M_B^2 \leq 2.1$ GeV². Accordingly, the mass of the $J_{0^{++}}^D$ state is extracted as:

$$M_{0^{++}}^D = (2.66 \pm 0.14) \text{ GeV}. \quad (30)$$

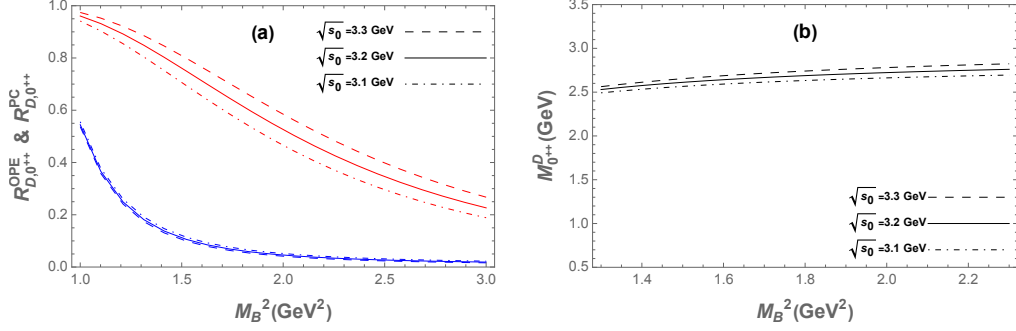


FIG. 5: (a) The ratios $R_{D,0^{++}}^{OPE}$ and $R_{D,0^{++}}^{PC}$ as functions of the Borel parameter M_B^2 for different values of $\sqrt{s_0}$ for current (4), where blue lines represent $R_{D,0^{++}}^{OPE}$ and red lines denote $R_{D,0^{++}}^{PC}$. (b) The mass of 0^{++} fully strange tetraquark state as a function of the Borel parameter M_B^2 for different values of $\sqrt{s_0}$.

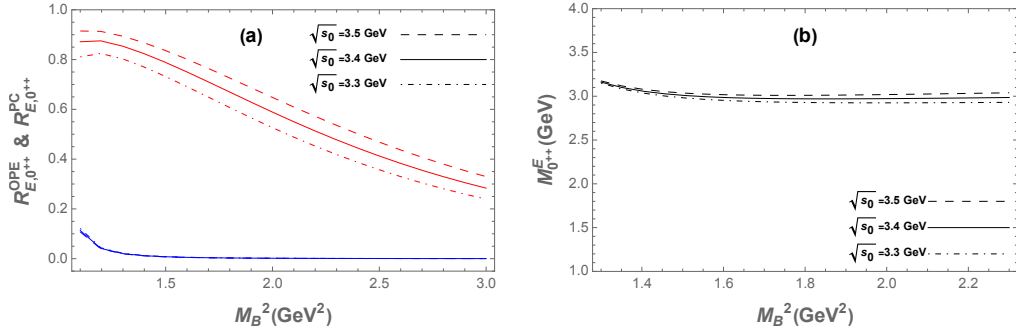


FIG. 6: (a) The ratios $R_{E,0^{++}}^{OPE}$ and $R_{E,0^{++}}^{PC}$ as functions of the Borel parameter M_B^2 for different values of $\sqrt{s_0}$ for current (5), where blue lines represent $R_{E,0^{++}}^{OPE}$ and red lines denote $R_{E,0^{++}}^{PC}$. (b) The mass of 0^{++} fully strange tetraquark state as a function of the Borel parameter M_B^2 for different values of $\sqrt{s_0}$.

For the current $J_{0^{++}}^E$, the OPE convergence and pole contribution ratios are displayed in Fig.6(a), while the corresponding mass curves are shown in Fig.6(b) for values of the continuum threshold: $\sqrt{s_0} = 3.3, 3.4$, and 3.5 GeV. A reliable and stable mass prediction is achieved within the Borel window $1.4 \leq M_B^2 \leq 2.2$ GeV², satisfying both the OPE convergence and pole dominance criteria. Consequently, the mass of the fully strange tetraquark state associated with the current $J_{0^{++}}^D$ is extracted to be:

$$M_{0^{++}}^E = (3.00 \pm 0.08) \text{ GeV}. \quad (31)$$

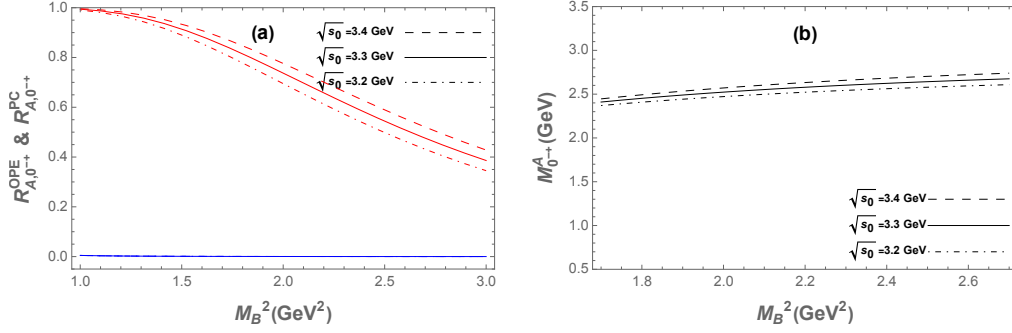


FIG. 7: (a) The ratios $R_{A,0-+}^{OPE}$ and $R_{A,0-+}^{PC}$ as functions of the Borel parameter M_B^2 for different values of $\sqrt{s_0}$ for current (6), where blue lines represent $R_{A,0-+}^{OPE}$ and red lines denote $R_{A,0-+}^{PC}$. (b) The mass of 0^{-+} fully strange tetraquark state as a function of the Borel parameter M_B^2 for different values of $\sqrt{s_0}$.

For the current J_{0-+}^A , we investigate the behavior of the OPE convergence ratio $R_{A,0-+}^{OPE}$ and the pole contribution ratio $R_{A,0-+}^{PC}$ for several values of the continuum threshold parameter $\sqrt{s_0} = 3.2, 3.3$, and 3.4 GeV, as shown in Fig.7(a). The mass dependence on the Borel parameter M_B^2 . From these plots, an optimal Borel window is determined to be $1.8 \leq M_B^2 \leq 2.6$ GeV², within which the operator product expansion shows sufficient convergence and the pole contribution exceeds the minimal requirement, ensuring the validity of the QCD sum rule analysis. Within this reliable working region, the extracted mass of the fully strange tetraquark state associated with the current J_{0-+}^A is obtained as:

$$M_{0-+}^A = (2.57 \pm 0.16) \text{ GeV}. \quad (32)$$

For the current J_{0-+}^B , the behavior of the OPE convergence and the pole contribution ratio is illustrated in Fig.8(a), while the dependence of the extracted mass M_{0-+}^B on the Borel parameter M_B^2 is shown in Fig.8(b). The analysis is performed with three representative values of the continuum threshold: $\sqrt{s_0} = 3.4, 3.5$, and 3.6 GeV. A stable Borel window is identified as $1.6 \leq M_B^2 \leq 2.4$ GeV², within which the OPE shows good convergence and the pole contribution remains above the required lower bound, ensuring the reliability of the QCD sum rule analysis. Accordingly, the mass of the fully strange tetraquark state associated with the current J_{0-+}^B is determined to be:

$$M_{0-+}^B = (2.57 \pm 0.16) \text{ GeV}. \quad (33)$$

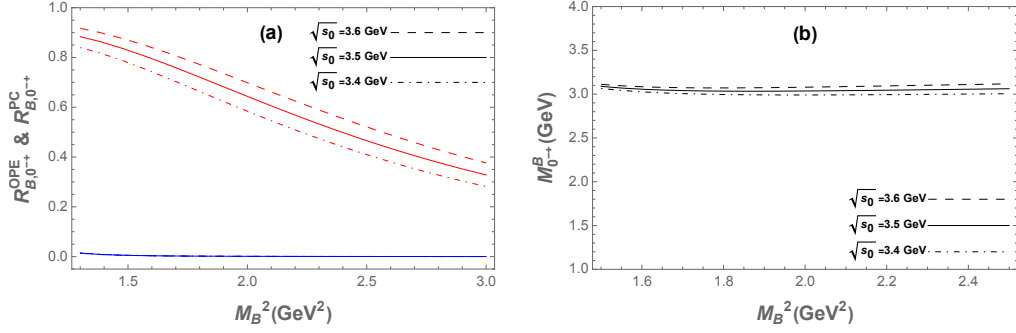


FIG. 8: (a) The ratios $R_{B,0^{++}}^{OPE}$ and $R_{B,0^{++}}^{PC}$ as functions of the Borel parameter M_B^2 for different values of $\sqrt{s_0}$ for current (7), where blue lines represent $R_{B,0^{++}}^{OPE}$ and red lines denote $R_{B,0^{++}}^{PC}$. (b) The mass of 0^{++} fully strange tetraquark state as a function of the Borel parameter M_B^2 for different values of $\sqrt{s_0}$.

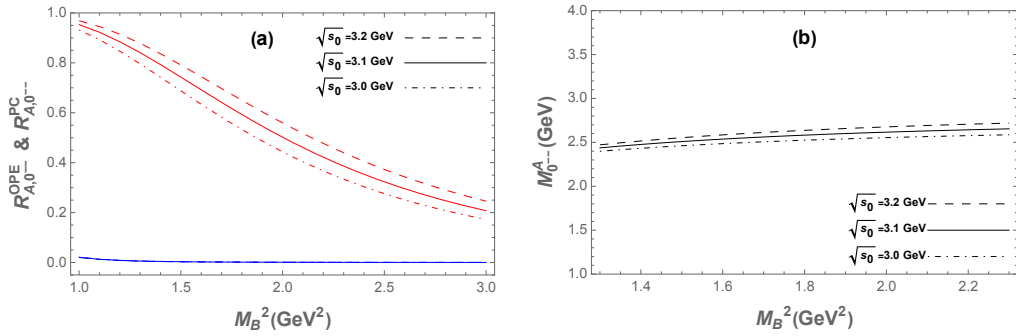


FIG. 9: (a) The ratios $R_{A,0^{--}}^{OPE}$ and $R_{A,0^{--}}^{PC}$ as functions of the Borel parameter M_B^2 for different values of $\sqrt{s_0}$ for current (8), where blue lines represent $R_{A,0^{--}}^{OPE}$ and red lines denote $R_{A,0^{--}}^{PC}$. (b) The mass of 0^{--} fully strange tetraquark state as a function of the Borel parameter M_B^2 for different values of $\sqrt{s_0}$.

For the current $J_{0^{--}}^A$, we display the behavior of the OPE convergence ratio $R_{A,0^{--}}^{OPE}$ and the pole contribution ratio $R_{A,0^{--}}^{PC}$ as functions of the Borel parameter M_B^2 in Fig.9(a), for three representative values of the continuum threshold $\sqrt{s_0} = 3.0, 3.1$, and 3.2 GeV. The corresponding mass curves are shown in Fig.9(b). From these analyses, an appropriate Borel window is identified to be $1.4 \leq M_B^2 \leq 2.1$ GeV², in which the operator product expansion demonstrates good convergence and the pole contribution exceeds 50%, satisfying the standard criteria of QCD sum rule applications. Within this optimal region, the mass of

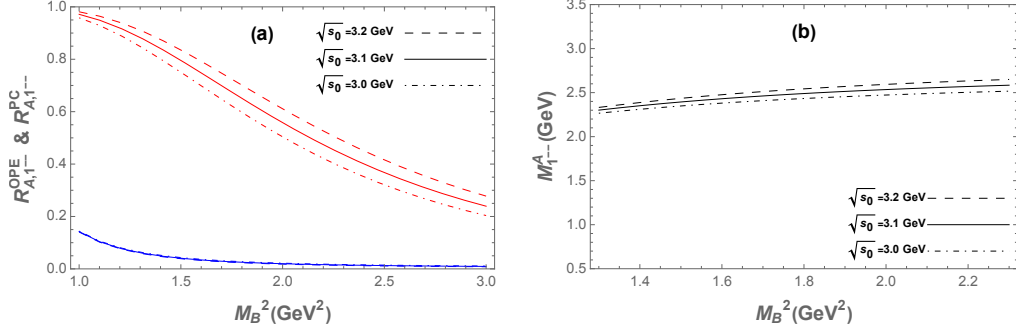


FIG. 10: (a) The ratios $R_{A,1--}^{OPE}$ and $R_{A,1--}^{PC}$ as functions of the Borel parameter M_B^2 for different values of $\sqrt{s_0}$ for current (9), where blue lines represent $R_{A,1--}^{OPE}$ and red lines denote $R_{A,1--}^{PC}$. (b) The mass of 1^{--} fully strange tetraquark state as a function of the Borel parameter M_B^2 for different values of $\sqrt{s_0}$.

the current J_{0--}^A fully strange tetraquark state is extracted as:

$$M_{0--}^A = (2.46 \pm 0.13) \text{ GeV}. \quad (34)$$

For the current J_{1--}^A , we present the OPE convergence ratio $R_{A,1--}^{OPE}$ and the pole contribution ratio $R_{A,1--}^{PC}$ as functions of the Borel parameter M_B^2 in Fig.10(a), for several values of the continuum threshold $\sqrt{s_0} = 2.8, 2.9$, and 3.0 GeV. The corresponding Borel curves for the extracted mass M_{1--}^A are shown in Fig.10(b). From these results, a stable mass plateau is observed within the Borel window $1.4 \leq M_B^2 \leq 2.1$ GeV², where both OPE convergence and pole dominance are reasonably satisfied. Within this reliable Borel region, the mass of fully strange tetraquark state associated with the current J_{1--}^A is determined to be:

$$M_{1--}^A = (2.46 \pm 0.15) \text{ GeV}. \quad (35)$$

For the current J_{1--}^B , the convergence of the operator product expansion and the dominance of the pole contribution are illustrated in Fig.11(a), with continuum thresholds $\sqrt{s_0} = 3.0, 3.1$, and 3.2 GeV. The extracted mass M_{1--}^B as a function of the Borel parameter M_B^2 is shown in Fig.11(b). A stable plateau is achieved in the range $1.3 \leq M_B^2 \leq 2.0$ GeV², satisfying the QCD sum rule criteria. Accordingly, the mass of the tetraquark state is obtained as:

$$M_{1--}^B = (2.59 \pm 0.09) \text{ GeV}. \quad (36)$$

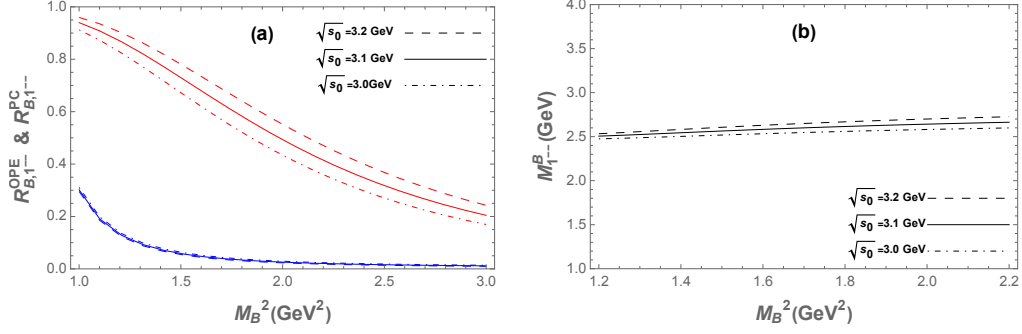


FIG. 11: (a) The ratios $R_{B,1--}^{OPE}$ and $R_{B,1--}^{PC}$ as functions of the Borel parameter M_B^2 for different values of $\sqrt{s_0}$ for current (10), where blue lines represent $R_{B,1--}^{OPE}$ and red lines denote $R_{B,1--}^{PC}$. (b) The mass of 1^{--} fully strange tetraquark state as a function of the Borel parameter M_B^2 for different values of $\sqrt{s_0}$.

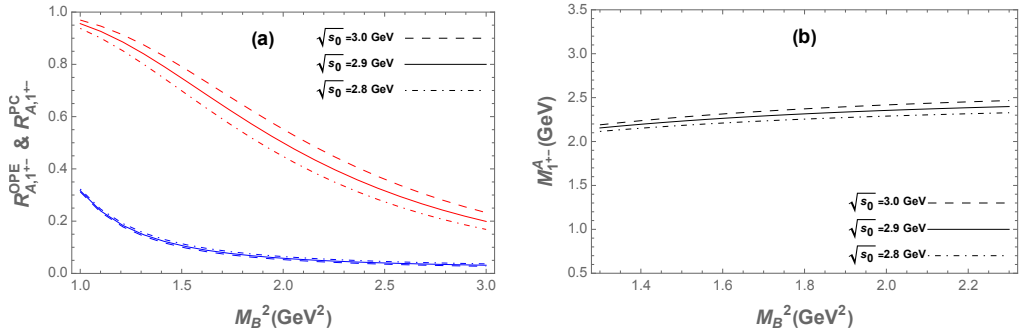


FIG. 12: (a) The ratios $R_{A,1+-}^{OPE}$ and $R_{A,1+-}^{PC}$ as functions of the Borel parameter M_B^2 for different values of $\sqrt{s_0}$ for current (11), where blue lines represent $R_{A,1+-}^{OPE}$ and red lines denote $R_{A,1+-}^{PC}$. (b) The mass of 1^{+-} fully strange tetraquark state as a function of the Borel parameter M_B^2 for different values of $\sqrt{s_0}$.

For the current J_{1+-}^A , the OPE convergence and the pole contribution ratios are plotted in Fig.12(a), while Fig.12(b) displays the extracted mass with $\sqrt{s_0} = 2.8, 2.9$, and 3.0 GeV. A reasonable Borel window is found to be $1.4 \leq M_B^2 \leq 2.1$ GeV², within which the sum rules remain valid. The mass extracted is:

$$M_{1+-}^A = (2.29 \pm 0.14) \text{ GeV}. \quad (37)$$

The OPE convergence and pole dominance for the current J_{1+-}^B are examined in Fig.13(a),

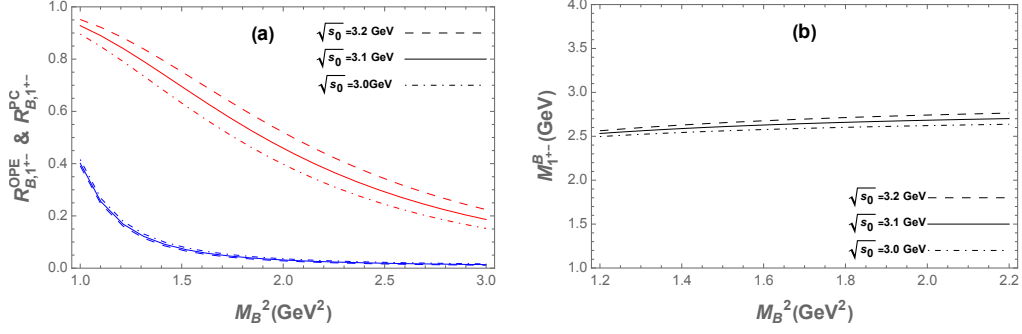


FIG. 13: (a) The ratios $R_{B,1+-}^{OPE}$ and $R_{B,1+-}^{PC}$ as functions of the Borel parameter M_B^2 for different values of $\sqrt{s_0}$ for current (12), where blue lines represent $R_{B,1+-}^{OPE}$ and red lines denote $R_{B,1+-}^{PC}$. (b) The mass of 1^{+-} fully strange tetraquark state as a function of the Borel parameter M_B^2 for different values of $\sqrt{s_0}$.

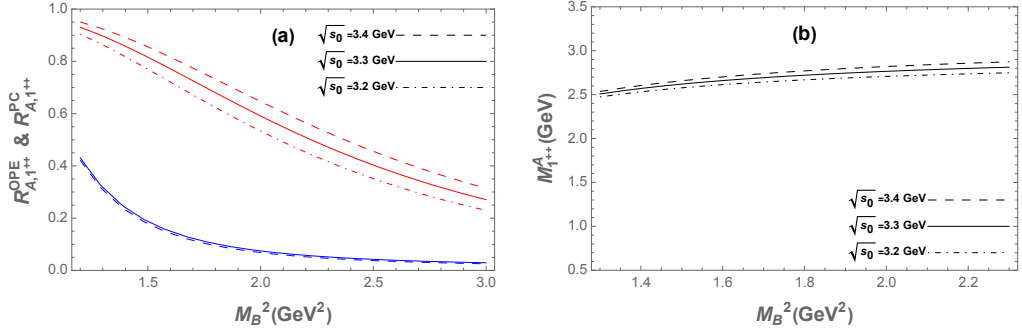


FIG. 14: (a) The ratios $R_{A,1++}^{OPE}$ and $R_{A,1++}^{PC}$ as functions of the Borel parameter M_B^2 for different values of $\sqrt{s_0}$ for current (13), where blue lines represent $R_{A,1++}^{OPE}$ and red lines denote $R_{A,1++}^{PC}$. (b) The mass of 1^{++} fully strange tetraquark state as a function of the Borel parameter M_B^2 for different values of $\sqrt{s_0}$.

and the mass Borel curves are shown in Fig.13(b), using $\sqrt{s_0} = 3.0, 3.1$, and 3.2 GeV. The Borel window $1.3 \leq M_B^2 \leq 2.0$ GeV² supports a reliable extraction of the mass:

$$M_{1+-}^B = (2.63 \pm 0.11) \text{ GeV}. \quad (38)$$

The current J_{1++}^A is analyzed similarly. As shown in Fig. 14(a) and (b), the sum rule analysis with $\sqrt{s_0} = 3.2, 3.3$, and 3.4 GeV yields a stable prediction within the Borel window

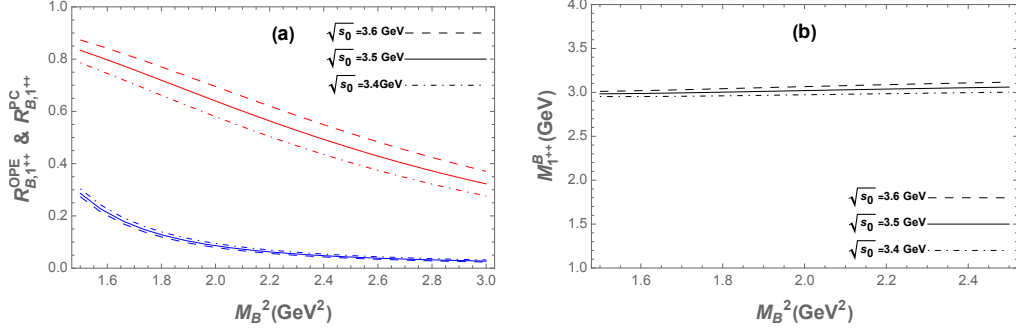


FIG. 15: (a) The ratios $R_{B,1^{++}}^{OPE}$ and $R_{B,1^{++}}^{PC}$ as functions of the Borel parameter M_B^2 for different values of $\sqrt{s_0}$ for current (14), where blue lines represent $R_{B,1^{++}}^{OPE}$ and red lines denote $R_{B,1^{++}}^{PC}$. (b) The mass of 1^{++} fully strange tetraquark state as a function of the Borel parameter M_B^2 for different values of $\sqrt{s_0}$.

$1.5 \leq M_B^2 \leq 2.2 \text{ GeV}^2$. The resulting mass of the corresponding tetraquark state is:

$$M_{1^{++}}^A = (2.72 \pm 0.14) \text{ GeV}. \quad (39)$$

Finally, for the current $J_{1^{++}}^B$, the corresponding OPE and pole contribution behavior is shown in Fig.15(a), and the Borel stability is verified in Fig.15(b). Using $\sqrt{s_0} = 3.4, 3.5$, and 3.6 GeV , we identify a valid Borel window in the range $1.7 \leq M_B^2 \leq 2.4 \text{ GeV}^2$, leading to the mass prediction:

$$M_{1^{++}}^B = (3.03 \pm 0.08) \text{ GeV}. \quad (40)$$

The uncertainties in the mass predictions presented in Eqs.(27)–(40) primarily arise from the variations in input parameters, including the quark masses, vacuum condensates, and the continuum threshold parameter $\sqrt{s_0}$. For clarity and ease of reference, the extracted mass values, together with the corresponding continuum thresholds and Borel windows, are summarized in Table I.

IV. DECAY ANALYSIS OF FULLY STRANGE TETRAQUARKS

To finally ascertain these fully strange tetraquark states, the straightforward procedure is to reconstruct them from their decay products, though the detailed characters still ask for

TABLE I: The continuum thresholds, Borel parameters, and predicted masses of fully strange tetraquark states.

J^{PC}	Current	$\sqrt{s_0}$ (GeV)	M_B^2 (GeV ²)	M^X (GeV)
0^{++}	A	2.9 ± 0.1	$1.4 - 2.2$	2.35 ± 0.15
	B	2.9 ± 0.1	$1.4 - 2.1$	2.24 ± 0.16
	C	3.1 ± 0.1	$1.4 - 2.1$	2.50 ± 0.14
	D	3.1 ± 0.1	$1.4 - 2.1$	2.66 ± 0.14
	E	3.4 ± 0.1	$1.4 - 2.2$	3.00 ± 0.08
0^{-+}	A	3.3 ± 0.1	$1.8 - 2.6$	2.57 ± 0.16
	B	3.5 ± 0.1	$1.6 - 2.4$	3.07 ± 0.05
0^{--}	A	3.1 ± 0.1	$1.4 - 2.1$	2.46 ± 0.13
1^{--}	A	2.9 ± 0.1	$1.4 - 2.1$	2.46 ± 0.15
	B	3.1 ± 0.1	$1.3 - 2.0$	2.59 ± 0.09
1^{+-}	A	2.9 ± 0.1	$1.4 - 2.1$	2.29 ± 0.14
	B	3.1 ± 0.1	$1.3 - 2.0$	2.63 ± 0.11
1^{++}	A	3.3 ± 0.1	$1.5 - 2.2$	2.72 ± 0.14
	B	3.5 ± 0.1	$1.7 - 2.4$	3.03 ± 0.08

more investigation. The decay properties of fully strange tetraquark states strongly depend on their quantum numbers J^{PC} , internal structure, and available phase space. Below, we briefly analyze the dominant and allowed decay channels for each quantum number:

1. For $J^{PC} = 0^{++}$ states. The scalar channel can decay via S-wave into two pseudoscalar or two vector mesons. Possible dominant decay modes include: $\phi\phi$, $\eta\eta$, $\eta'\eta'$, $\eta\eta'$, and $K\bar{K}$ channels. These are all OZI-allowed and likely lead to relatively broad widths, depending on the mass and phase space.
2. For $J^{PC} = 0^{-+}$ states. Being a pseudoscalar state, its decays typically proceed via P-wave into: $\phi\eta$, $\phi\eta'$, and $K\bar{K}^*$ channels. These modes are sensitive to angular momentum and available energy. If the mass is close to threshold, the width may be narrow.
3. For $J^{PC} = 0^{--}$ states. This is an exotic quantum number not accessible by con-

ventional $q\bar{q}$ mesons. Its decays are constrained and potentially suppressed. Allowed multi-body or radiative decays include: $\phi\eta\pi$ and $\eta\eta\gamma$ channels. Due to its exotic nature and limited phase space, this state may be relatively narrow and easier to identify experimentally.

4. For $J^{PC} = 1^{--}$ states. This vector state can be directly produced in e^+e^- collisions. Its dominant decays are typically: $\phi\eta$, $\phi\eta'$, $K\bar{K}$, and $K^*\bar{K}$ channels.
5. For $J^{PC} = 1^{+-}$ states. This axial-vector state can decay via: $\phi\eta$, $\phi\eta'$, and $K\bar{K}^*$ channels.
6. For $J^{PC} = 1^{++}$ states. Similar to the 1^{+-} case but with different parity, it can decay into: $\phi\eta$ and $K^*\bar{K}$ channels. The partial widths and branching ratios are sensitive to internal structure and coupling strengths.

The decay channels of fully strange tetraquarks offer clear experimental signatures, especially through final states such as $\phi\phi$, $\phi\eta$, and $K\bar{K}^*$. Exotic quantum number states like 0^{--} stand out due to their unusual decay modes and suppressed widths, making them key targets for discovery. Future searches at BESIII, Belle II, and LHCb can test these predictions by analyzing invariant mass spectra in strange-rich final states.

V. SUMMARY

In this work, we have systematically investigated the mass spectrum of fully strange tetraquark states ($ss\bar{s}\bar{s}$) in molecular configurations with quantum numbers $J^{PC} = 0^{++}$, 0^{-+} , 0^{--} , 1^{--} , 1^{+-} , and 1^{++} within the framework of QCD sum rules (QCDSR). By constructing appropriate interpolating currents and applying standard QCDSR techniques we obtained mass predictions for each quantum number channel. The resulting masses fall within the range of approximately 2.08 to 3.12 GeV, depending on the quantum numbers and the interpolating currents used, which are summarized in Table I. Notably, the mass of the $J^{PC} = 1^{+-}$ state shows good agreement with the $X(2300)$ resonance recently reported by the BESIII Collaboration, hinting at a possible exotic tetraquark interpretation. Further-

more, the possible decay modes of these fully strange tetraquark states have been analyzed in detail.

Among these, particular attention is paid to the exotic $J^{PC} = 0^{--}$ channel, which is forbidden in conventional quark-antiquark meson configurations and thus serves as a strong indicator of multiquark or gluonic degrees of freedom. The observation of a state with such quantum numbers would provide compelling evidence for the existence of non-conventional hadrons and offer a direct window into the exotic sector of QCD.

These findings not only enrich the theoretical understanding of multiquark states but also offer concrete and testable predictions for future experimental searches at BESIII, Belle II, LHCb, and other high energy facilities. Owing to its flavor-pure composition and the absence of mixing with light or heavy quarks, the fully strange tetraquark system provides a particularly clean and ideal environment for probing novel hadronic structures and exploring the nonperturbative dynamics of QCD.

Acknowledgments

This work was supported in part by Specific Fund of Fundamental Scientific Research Operating Expenses for Undergraduate Universities in Liaoning Province under Grants No. LJ212410165019 and the National Natural Science Foundation of China under Grants No. 12147214.

-
- [1] M. Gell-Mann, Phys. Lett. **8**, 214 (1964).
 - [2] G. Zweig, Report No. CERN-TH-401.
 - [3] S. K. Choi *et al.* [Belle Collaboration], Phys. Rev. Lett. **91**, 262001 (2003).
 - [4] M. Ablikim *et al.* [BESIII], Phys. Rev. Lett. **106**, 072002 (2011).
 - [5] J. Z. Bai *et al.* [BES], Phys. Rev. Lett. **91**, 022001 (2003).
 - [6] M. Ablikim *et al.* [BES], Phys. Rev. Lett. **95**, 262001 (2005).
 - [7] M. Ablikim *et al.* [BESIII], Chin. Phys. C **34**, 421 (2010).
 - [8] M. Ablikim *et al.* [BESIII], Eur. Phys. J. C **80**, 746 (2020).

- [9] M. Ablikim *et al.* [BESIII], Phys. Rev. D **93**, 112011 (2016).
- [10] M. Ablikim *et al.* [BESIII], Phys. Rev. Lett. **124**, 112001 (2020).
- [11] M. Ablikim *et al.* [BESIII], Phys. Rev. D **95**, 052003 (2017).
- [12] M. Ablikim *et al.* [BESIII], Phys. Rev. D **97**, 032013 (2018).
- [13] M. Ablikim *et al.* [BESIII], Phys. Rev. Lett. **124**, 032002 (2020).
- [14] M. Ablikim *et al.* [BESIII], Phys. Rev. Lett. **134**, 191901 (2025).
- [15] Q. Li, L. C. Gui, M. S. Liu, Q. F. Lü and X. H. Zhong, Chin. Phys. C **45**, 023116 (2021).
- [16] L. Y. Xiao, X. Z. Weng, X. H. Zhong and S. L. Zhu, Chin. Phys. C **43**, 113105 (2019).
- [17] S. Ishida and K. Yamada, Phys. Rev. D **35**, 265 (1987).
- [18] D. Ebert, R. N. Faustov and V. O. Galkin, Phys. Rev. D **79**, 114029 (2009).
- [19] J. Oudichhya, K. Gandhi and A. K. Rai, Phys. Rev. D **108**, 014034 (2023).
- [20] L. M. Wang, J. Z. Wang, S. Q. Luo, J. He and X. Liu, Phys. Rev. D **101**, 034021 (2020).
- [21] K. Chen, C. Q. Pang, X. Liu and T. Matsuki, Phys. Rev. D **91**, 074025 (2015).
- [22] F. X. Liu, M. S. Liu, X. H. Zhong and Q. Zhao, Phys. Rev. D **103**, 016016 (2021).
- [23] M.A. Shifman, A.I. Vainshtein and V.I. Zakharov, Nucl. Phys. **B147**, 385 (1979); *ibid*, Nucl. Phys. **B147**, 448 (1979).
- [24] B. D. Wan, S. Q. Zhang and C. F. Qiao, Phys. Rev. D **106**, 074003 (2022).
- [25] R. M. Albuquerque, arXiv:1306.4671 [hep-ph].
- [26] Z. G. Wang and T. Huang, Phys. Rev. D **89**, 054019 (2014).
- [27] R. D. Matheus, S. Narison, M. Nielsen and J. M. Richard, Phys. Rev. D **75**, 014005 (2007).
- [28] C. Y. Cui, Y. L. Liu and M. Q. Huang, Phys. Rev. D **85**, 074014 (2012).
- [29] L. Tang, B. D. Wan, K. Maltman and C. F. Qiao, Phys. Rev. D **101**, 094032 (2020).
- [30] P. Colangelo and A. Khodjamirian, in *At the frontier of particle physics / Handbook of QCD*, edited by M. Shifman (World Scientific, Singapore, 2001), arXiv:hep-ph/0010175.
- [31] J. Govaerts, L. J. Reinders, H. R. Rubinstein and J. Weyers, Nucl. Phys. B **258**, 215-229 (1985).
- [32] L. J. Reinders, H. Rubinstein and S. Yazaki, Phys. Rept. **127**, 1 (1985).
- [33] S. Narison, World Sci. Lect. Notes Phys. **26** 1 (1989).
- [34] C. M. Tang, Y. C. Zhao and L. Tang, Phys. Rev. D **105**, 114004 (2022).
- [35] C. F. Qiao and L. Tang, Phys. Rev. Lett. **113**, 221601 (2014).
- [36] C. F. Qiao and L. Tang, Eur. Phys. J. C **74**, 2810 (2014).
- [37] L. Tang and C. F. Qiao, Nucl. Phys. B **904**, 282-296 (2016).
- [38] C. F. Qiao and L. Tang, EPL **107**, 31001 (2014).
- [39] B. D. Wan, L. Tang and C. F. Qiao, Eur. Phys. J. C **80**, 121 (2020).
- [40] C. M. Tang, C. G. Duan and L. Tang, Eur. Phys. J. C **84**, 743 (2024).

- [41] C. F. Qiao and L. Tang, Eur. Phys. J. C **74**, 3122 (2014).
- [42] C. M. Tang, C. G. Duan, L. Tang and C. F. Qiao, Eur. Phys. J. C **85**, 396 (2025).
- [43] B. D. Wan and C. F. Qiao, Nucl. Phys. B **968**, 115450 (2021).
- [44] B. D. Wan and C. F. Qiao, Phys. Lett. B **817**, 136339 (2021).
- [45] S. N. Li and L. Tang, [arXiv:2404.11145 [hep-ph]].
- [46] B. D. Wan, S. Q. Zhang and C. F. Qiao, Phys. Rev. D **105**, 014016 (2022).
- [47] Y. C. Zhao, C. M. Tang and L. Tang, Eur. Phys. J. C **83**, 654 (2023).
- [48] S. Q. Zhang, B. D. Wan, L. Tang and C. F. Qiao, Phys. Rev. D **106**, 074010 (2022).
- [49] B. D. Wan and C. F. Qiao, [arXiv:2208.14042 [hep-ph]].
- [50] F. H. Yin, W. Y. Tian, L. Tang and Z. H. Guo, Eur. Phys. J. C **81**, 818 (2021).
- [51] B. D. Wan, Eur. Phys. J. C **84**, 760 (2024).
- [52] L. Tang and C. F. Qiao, Eur. Phys. J. C **76**, 558 (2016).
- [53] B. C. Yang, L. Tang and C. F. Qiao, Eur. Phys. J. C **81**, 324 (2021).
- [54] B. D. Wan, Nucl. Phys. B **1004**, 116538 (2024).
- [55] B. D. Wan and H. T. Xu, Chin. Phys. C **48**, 093103 (2024).
- [56] B. D. Wan and Y. R. Wang, Eur. Phys. J. A **60**, 179 (2024).
- [57] B. D. Wan and S. Yang, Eur. Phys. J. A **61**, 11 (2025).
- [58] W. S. Zhang and L. Tang, [arXiv:2412.11531 [hep-ph]].
- [59] S. Q. Zhang and C. F. Qiao, Phys. Rev. D **108**, 074017 (2023).
- [60] S. Q. Zhang, X. H. Zhang and C. F. Qiao, JHEP **06**, 122 (2024).
- [61] S. Q. Zhang and C. F. Qiao, Phys. Rev. D **110**, 114040 (2024).
- [62] X. H. Zhang, S. Q. Zhang and C. F. Qiao, Eur. Phys. J. C **85**, 693 (2025).